



King Saud University
Arabian Journal of Chemistry

www.ksu.edu.sa
www.sciencedirect.com



ORIGINAL ARTICLE

Design, synthesis and biological activity of novel chalcone derivatives containing indole



Die Hu, Nian Zhang, Yuanquan Zhang, Chunmei Yuan, Chenyu Gong, Yuanxiang Zhou, Wei Xue*

National Key Laboratory of Green Pesticide, Key Laboratory of Green Pesticide and Agricultural Bioengineering, Ministry of Education, Center for R&D of Fine Chemicals of Guizhou University, Guiyang 550025, China

Received 4 November 2022; accepted 1 March 2023

Available online 8 March 2023

KEYWORDS

Chalcone derivatives;
Indole;
Antiviral activity;
Bacteriostatic activity;
Mechanism of action

Abstract In this study, 24 chalcone derivatives containing indole were designed and synthesized. Some of the target compounds exhibited significant antiviral and antibacterial effects. The results of EC₅₀ test against tobacco mosaic virus showed that the EC₅₀ value of curative activity of **D11** was 107.4 µg/mL, which was better than the commercial drug ningnanmycin 311.5 µg/mL, and the EC₅₀ value of protective activity of **D16** was 106.6 µg/mL, which was superior to ningnanmycin 205.4 µg/mL, the inactivated activity of **D11** was comparable to that of ningnanmycin. Microscale thermophoresis experiments demonstrated **D11** ($K_d = 0.0030 \pm 0.0014$ µmol/L) had a stronger binding ability with tobacco mosaic virus capsid protein (TMV-CP), which was much higher than that of ningnanmycin ($K_d = 2.6062 \pm 1.1767$ µmol/L). Molecular docking results showed **D11** had a significantly higher affinity with TMV protein than ningnanmycin. In addition, the malondialdehyde (MDA), peroxidase (POD), succinate dehydrogenase content (SDH) assay showed **D11** could improve the disease resistance of tobacco. The results of bacterial inhibition activity showed that the EC₅₀ value of **D23** against *Xoo* was 50.3 µg/mL, which was better than the commercial drugs thio-diazole copper (79.8 µg/mL) and bismertiazol (106.2 µg/mL), the bacterial inhibition activity of **D23** was verified by scanning electron microscopy.

© 2023 The Author(s). Published by Elsevier B.V. on behalf of King Saud University. This is an open access article under the CC BY-NC-ND license (<http://creativecommons.org/licenses/by-nc-nd/4.0/>).

1. Introduction

Our country is a large agricultural country with a long history, in the process of agricultural development, the agricultural economy has made remarkable achievements (Xu et al., 2021; Yan et al., 2021). In recent years, achieving high quality and high yield of crops is the key to consolidate and strengthen the agricultural economy of China (Wu et al., 2022; Chao, 2019). But as agriculture continues to develop, many problems and challenges have been gradually revealed with

respect to crops (Mariana and Octávio, 2022). The increasing number of some crop diseases caused by plant viruses, phytopathogenic bacteria, etc. (Marqués et al., 2022; Liu et al., 2021), has seriously affected the quality of agricultural products and the number of varieties, so crop disease control has become a requirement of the times to supplement the shortcomings of the agricultural economy. The use of pesticides is the most effective method to prevent and control crop diseases, but problems such as enhanced drug resistance, pesticide residues and environmental pollution have also emerged subsequently (Li

* Corresponding author.

E-mail address: wxue@gzu.edu.cn (W. Xue).

et al., 2021; Claudio et al., 2018; Zhao et al., 2018). Therefore, it is important to research new commercial pesticides with high efficiency, low toxicity and environmental protection (Jiang et al., 2020).

Chalcone is a precursor of flavonoid synthesis in plants with the chemical structural formula 1,3-diphenyl-2-propen-1-one, its derivatives are mainly concentrated in parts A, B and C (Fig. 1) (Li et al., 2022; Nadia et al., 2022; Chandrabose et al., 2014) and are widely found in vegetables, soybeans, fruits, spices, tea and other plants (Hiroyuki et al., 2003; Ye et al., 2016). Chalcone and its derivatives have been found to possess a variety of biological activities, such as antiviral (Fu et al., 2020), antibacterial (Chen et al., 2020; Zhou et al., 2022), anticancer (Yang et al., 2021), antioxidant (Bale et al., 2021; Zahrani et al., 2020), anthelmintic (José et al., 2018), and anti-inflammatory (Nurkenov et al., 2019; Ibrahim et al., 2021). In view of this, chalcones have also been successively used in the synthesis of biopesticides, the domestically registered isobavachalcone is a plant-derived fungicide with chalcone structure extracted from the legume tonic (Guan et al., 2014). The design and synthesis of novel pesticides with excellent activity by introducing biologically active pharmacophore into the chalcone backbone has become a hot topic in the field of pesticide chemistry. Indole (Fig. 1) is an aromatic heterocyclic alkaloid found not only in natural plants such as jasmine, oleander, citrus, croton root and orange blossom (Qin et al., 2015; Wei et al., 2018; Ding et al., 2018), but also in many animals and marine organisms (Liu et al., 2017; Lin and Tan, 2018). Both indoles and their derivatives exhibit many biological activities, such as: antibacterial (Xu et al., 2017; Kang et al., 2020), antitumor (Palassini et al., 2017), antiviral (Xie et al., 2020; Wang et al., 2021), antioxidant (Quan and Adam, 2020), and anti-inflammatory (Liu et al., 2016). As extremely important heterocyclic skeletal pharmacophore, indoles are widely used in pharmaceuticals, pesticides, fragrances, dyes, and other research fields. Therefore, the exploration of indoles has been favored by many chemists and pharmacologists.

In order to find novel pesticide compounds with excellent antiviral and bacterial inhibition, 24 chalcone derivatives containing indole were synthesized according to the principle of active splicing in drug synthesis (Fig. 2 and Scheme 1). All target compounds were tested for antiviral and bacterial inhibition activities. The results of antiviral tests showed that the **D11** had excellent curative, protective and inactivated activities against tobacco mosaic virus. The Molecular docking, MST, MDA, POD and SDH assays were performed on **D11**, molecular docking and MST results showed **D11** had a strong binding ability with TMV-CP, the experiments of MDA, POD, SDH showed **D11** could improve the disease resistance of tobacco. In addition, the results of bacterial inhibition tests showed **D23** has excellent inhibitory effect on *Xoo*. SEM experiments were performed on **D23** to observe the effect of **D23** on *Xoo* cells. This study provides a useful guiding basis for the development of new pesticides.

2. Materials and methods

2.1. Instruments and chemicals

2.1.1. Instruments

The melting points were determined by using an XT-4 binocular microscope (Beijing, China) and uncorrected. ^1H , ^{13}C , and ^{19}F nuclear magnetic resonance (NMR) spectra were obtained



Fig. 1 The structures of chalcone and indole.

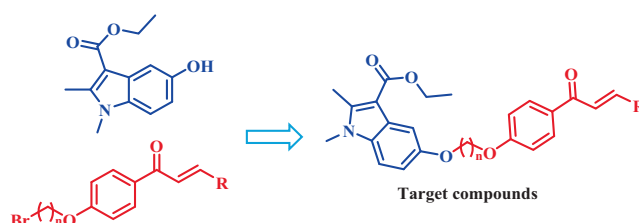


Fig. 2 Design of target compounds.

using JEOL-ECX500 (Tokyo, Japan) and Bruker 400 NMR spectrometer (Bruker Corporation, Germany). High-resolution mass spectrometry (HRMS) was conducted by using a Thermo Scientific Q Exactive (Thermo Scientific, Missouri, USA). The K_d values of compounds to TMV-CP were determined by NanoTemper Monolith NT.115 microscale thermophoresis instrument (München, Germany). Enzyme activity data were determined by MultiskanFC Microplate reader (Beijing, China).

2.1.2. Chemicals

Various reaction materials were purchased from Shanghai Titan Technology Co., Ltd (Shanghai, China). Bismertiazol, Thiodiazole copper and ningnanmycin were purchased from Shanghai Tansoole Platform (Shanghai, China). All chemical reagents and solvents are analytically pure. The enzyme activity kit was purchased from Beijing Solarbio Technology Co., Ltd (Beijing, China). Other chemical materials were purchased from Bositai Technology Co., Ltd (Chongqing, China).

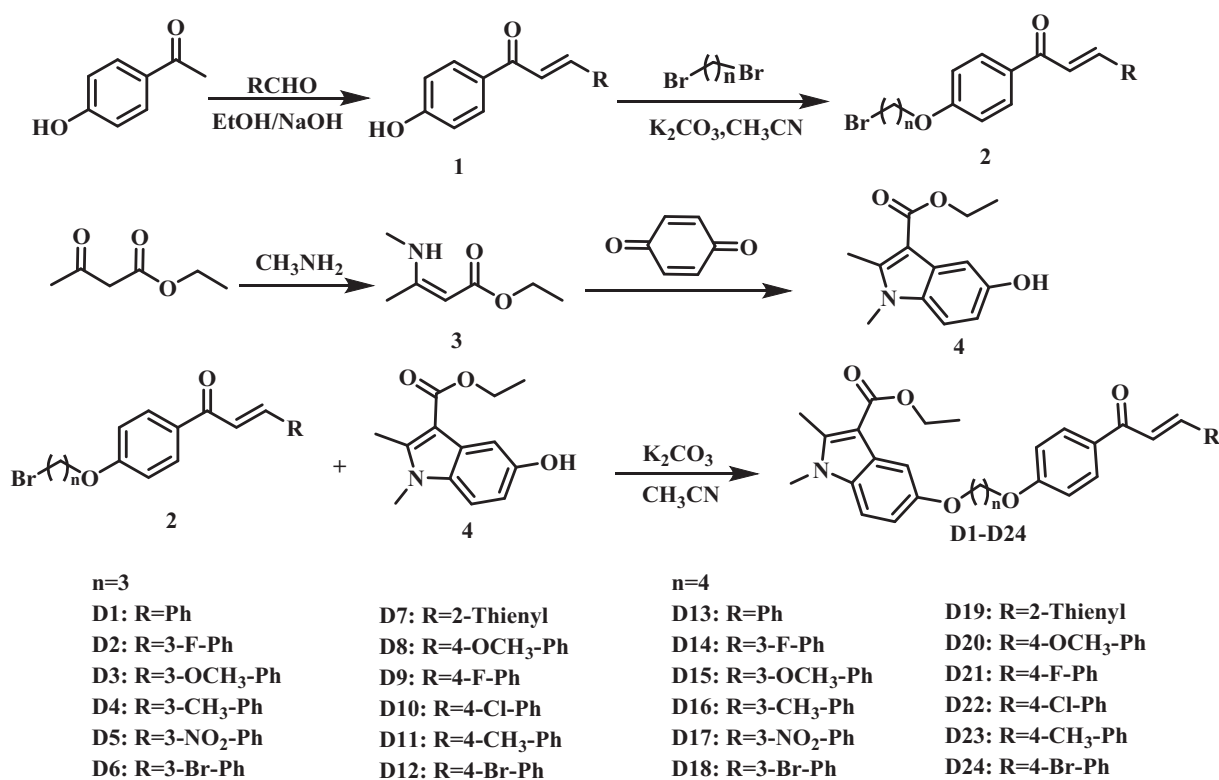
2.2. Synthesis

2.2.1. Synthesis of intermediates 1–4

Intermediates **1** and **2** were synthesized according to the method of the literature (Chen et al., 2020; Zhou et al., 2022). Intermediates **3** and **4** were synthesized according to the literature (Huang et al., 2019). The methylamine solution was slowly added to a round bottom flask containing ethyl acetoacetate, the reaction was carried out at room temperature for 3 h. After completion of the reaction, the organic phase was washed with water, and the organic phase was dried to obtain the pale-yellow liquid intermediate **3**. The *P*-benzoquinone, acetone and intermediate **3** were added to the reaction flask in sequence and reacted at 30 °C for 2 h. After concentrating under reduced pressure, acetone was recrystallized to obtain intermediate **4**.

2.2.2. Synthesis of target compounds **D1-D24**

Intermediate **4** (3.60 mmol), K_2CO_3 (9.00 mmol) and 30 mL CH_3CN were added to 100 mL round bottom flask, condense and reflux at 80 °C for 60 min. Intermediate **2** (3.0 mmol) was added to the reaction system, continue to heat and reflux the reaction for 8 h. The reaction system was concentrated under reduced pressure, and then pour into 500 mL of ice water, a white solid was precipitated. After standing for 60 min, the reaction system was filtered under reduced pressure and dried, the crude product was recrystallized with anhydrous ethanol. Finally, the target compounds **D1-D24** were purified by column chromatography (petroleum ether: ethyl acetate = 2:1, *v/v*).



Scheme 1 Synthetic route of compounds **D1-D24**.

2.3. Anti-TMV activity assay

According to the previously reported method in the literature (Peng et al., 2021). The antiviral activity of the compounds against TMV *in vivo* was tested at an agent concentration of 500 µg/mL. In addition, EC₅₀ values for against TMV were tested at concentrations of 500, 250, 125, 62.5 and 31.25 µg/mL. The commercial drug NNM was used as the control agent. Each measurement was repeated three times.

2.4. Microscale thermophoresis experiment (MST)

The interaction of the target compounds to TMV-CP was investigated by previously reported approach in the literature (Liu et al., 2022).

2.5. Molecular docking

The molecular docking of compound **D11** to TMV-CP was carried out according to the method reported in the literature (Ding et al., 2022). AutoDockTools and PyMOLWin software were used to simulate and validate the binding ability of target compounds to TMV proteins.

2.6. Defensive enzyme activity measurement

The defense enzyme activity of **D11** was tested according to the methods in the literature (Liu et al., 2022; Gan et al., 2021). *Nicotiana Tabacum* K326 was induced whole leaves in a green-

house with **D11** and a solvent (DMSO + 1% Tween water), where the solvent was used as a negative control (CK). After 12 h of induction, TMV was inoculated on the tobacco leaves and the leaves were collected on 1, 3, 5 and 7 d. Then added to liquid nitrogen to obtain CK, CK + TMV, **D11** and **D11** + TMV groups, which were ground into powder and measuring the enzyme activity content in the leaves according to the method in the kit instructions.

2.7. Determination of MDA content

The MDA content of TMV infected tobacco leaves treated with **D11** was tested according to the method described in the literature (Zhang et al., 2017). Tobacco leaves on 1, 3, 5 and 7 d were collected as samples and divided into CK, CK + TMV, **D11** and **D11** + TMV groups, subsequently the absorbance of each sample was measured at 532 nm and 600 nm according to the method described in the kit instructions, the MDA content was calculated by referring to the kit instructions.

2.8. Measurement of antibacterial activity

According to the literature (Tang et al., 2022), **D1-D24** were determined by a modified 96-well plate method against *Xoo*, *Xac*, *Psa* for their antibacterial activity. The corresponding concentration of DMSO solution was used as a negative control, the commercial drugs thiodiazole copper and bismethiazol were used as positive controls. Three parallel experiments were performed for each sample.

2.9. Scanning electron microscopy

SEM experiments were performed on the bacterial inhibition of **D23**, all methods were referred to previous literature (Peng et al., 2021).

3. Results and discussion

3.1. Chemistry

The **D1-D24** were synthesized according to the designed route of Scheme 1. All the target compounds were characterized by NMR and HRMS, the detailed data are in the Supporting Material.

3.2. Antiviral activity of **D1-D24** against TMV *in vivo*

The against TMV activity of the synthesized target compounds was determined at concentration of 500 $\mu\text{g}/\text{mL}$ with the half-leaf blight spot methods, the results are shown in Table 1, most of the compounds showed excellent against TMV activity, the curative activities of compounds **D11**, **D12**, **D15**, **D16**, **D18** and **D22** were 74.7, 65.8, 70.2, 65.9, 71.9 and 73.6%, which were superior to NNM 57.1%. The protective activities of compounds **D2**, **D4**, **D10**, **D11**, **D12**, **D16** and **D18** were 72.2, 71.3, 72.4, 73.6, 75.5, 77.0 and 74.1%, which were better than NNM 68.2%. The inhibition rate of inactivated activity of **D11** was 86.1%, which was comparable to that of NNM. Among them, the tobacco leaf morphology of **D11** against TMV *in vivo* is shown in Fig. 3. **D11** showed significant inhibition of TMV in both curative and protective activities, which was superior to the commercial drug NNM.

Based on the results of the initial screening, the EC_{50} values of some compounds against TMV were further tested and the results are shown in Table 2. The EC_{50} values of curative activity of **D11**, **D15**, and **D22** were 107.4, 108.4, and 104.0 $\mu\text{g}/\text{mL}$, which were better than that of NNM 311.5 $\mu\text{g}/\text{mL}$. The EC_{50} values of protective activity of **D2**, **D12**, and **D16** were 106.3, 114.8, and 106.6 $\mu\text{g}/\text{mL}$, which were better than NNM 205.4 $\mu\text{g}/\text{mL}$.

The structure–activity relationship (SAR) was analyzed according to the anti-TMV activities shown in Table 1. The target compounds showed better protective, curative and inactivated activities against TMV. when the number of C-atoms of brominated alkanes was $n = 3$ and R was an electron-giving substituted phenyl group. For example, the curative activity was **D11** (R = 4- CH_3 -Ph, 74.7%) > **D12** (R = 4-Br-Ph, 65.8%), the protective activity was **D11** (R = 4- CH_3 -Ph, 73.6%) > **D10** (R = 4-Cl-Ph, 72.4%) > **D9** (R = 4-F-Ph, 62.6%), the inactivated activity was **D11** (R = 4- CH_3 -Ph, 86.1%) > **D10** (R = 4-Cl-Ph, 78.2%). When the number of brominated alkane C atoms $n = 4$, R was halogen substituted phenyl, the target compounds showed higher protection and curative against TMV, such as curative activity **D22** (R = 4-Cl-Ph, 73.6%) > **D16** (R = 3- CH_3 -Ph, 65.9%), protective activity **D18** (R = 3-Br-Ph, 74.1%) > **D15** (R = 3-OCH₃-Ph, 56.6%).

In summary, **D11** ($n = 3$, R = 4- CH_3 -Ph) showed significant inhibitory activity against TMV in terms of curative, protective and inactivated activities, when $n = 4$, R was halogen-

Table 1 Antiviral activity of **D1-D24** against TMV at 500 $\mu\text{g}/\text{mL}$ *in vivo*.

Compounds	Curative activity (%) ^a	Protective activity (%) ^a	Inactivated activity (%) ^a
D1	63.6 ± 5.4	68.3 ± 1.8	71.3 ± 5.2
D2	50.9 ± 5.3	72.2 ± 2.6	72.5 ± 3.3
D3	56.4 ± 0.9	59.9 ± 1.3	70.9 ± 6.1
D4	41.1 ± 4.3	71.3 ± 3.6	74.8 ± 2.7
D5	43.3 ± 3.6	66.2 ± 0.8	62.9 ± 2.4
D6	50.6 ± 4.7	59.6 ± 1.7	66.9 ± 4.7
D7	52.9 ± 4.7	66.0 ± 3.0	61.6 ± 2.9
D8	31.3 ± 2.2	55.7 ± 1.6	55.5 ± 1.8
D9	62.6 ± 1.8	63.0 ± 6.4	72.5 ± 5.1
D10	59.0 ± 1.6	72.4 ± 1.7	78.2 ± 1.5
D11	74.7 ± 2.8	73.6 ± 2.1	86.1 ± 1.0
D12	65.8 ± 4.3	75.5 ± 0.7	58.7 ± 0.9
D13	47.4 ± 5.5	51.6 ± 5.4	41.4 ± 2.0
D14	38.3 ± 0.4	60.6 ± 4.5	56.7 ± 2.7
D15	70.2 ± 4.5	56.6 ± 2.5	80.9 ± 0.9
D16	65.9 ± 3.6	77.0 ± 3.2	84.5 ± 4.3
D17	43.9 ± 5.7	54.6 ± 1.5	60.3 ± 4.7
D18	71.9 ± 0.5	74.1 ± 1.7	72.9 ± 1.2
D19	45.2 ± 2.7	38.0 ± 3.3	55.4 ± 3.6
D20	65.4 ± 4.6	56.3 ± 3.1	57.3 ± 2.1
D21	62.0 ± 3.2	70.9 ± 0.3	57.4 ± 6.5
D22	73.6 ± 3.4	61.5 ± 2.2	54.6 ± 5.2
D23	58.2 ± 2.1	68.1 ± 4.6	55.0 ± 2.5
D24	58.7 ± 2.9	68.8 ± 3.5	64.4 ± 2.5
NNM ^b	57.1 ± 1.9	68.2 ± 1.6	91.8 ± 0.6

^a Average of three replicates, ^b The commercial antiviral agent. Ningnanmycin (NNM).

substituted phenyl, the protective and curative activities of the target compound against TMV were enhanced.

3.3. Binding ability of **D11**, **D13**, **D15** and NNM to TMV-CP

The results of MST study of **D11**, **D13**, **D15** and NNM to TMV-CP are shown in Fig. 4. The dissociation constants K_d values of **D11**, **D13**, **D15** and NNM for TMV-CP were 0.0030 ± 0.0014 $\mu\text{mol}/\text{L}$, 8.0268 ± 3.3977 $\mu\text{mol}/\text{L}$, 0.1371 ± 0.0310 $\mu\text{mol}/\text{L}$ and 2.6062 ± 1.1767 $\mu\text{mol}/\text{L}$. It is thus clear that **D11**, **D15** have better affinity for TMV-CP than NNM and much surpassed than **D13**. In summary, the magnitude of binding capacity with TMV-CP was **D11** > **D15** > NNM > **D13**. which was consistent with the results of the initial against TMV screening.

3.4. Molecular docking of compounds **D11**, **D13** and NNM with TMV-CP

The molecular docking results of **D11**, **D13** and NNM are shown in Table 3 and Fig. 5. **D11** formed two hydrogen bonds with TMV-CP, in which the indole carbonyl oxygen atom of **D11** formed a hydrogen bond with residue SER-215 (3.0 Å) of TMV-CP, the indole hydroxyl oxygen atom formed a hydrogen bond with residue ASP-70 (3.8 Å), the total binding free energy was -7.44 kcal/mol. Obviously, the more hydrogen bonds and the lower the binding free energy, the more stable the docking result. In supplement to this, **D11** also formed seven hydrophobic bonds with other residues, which provided a certain intermolecular force for **D11** and showed a significant

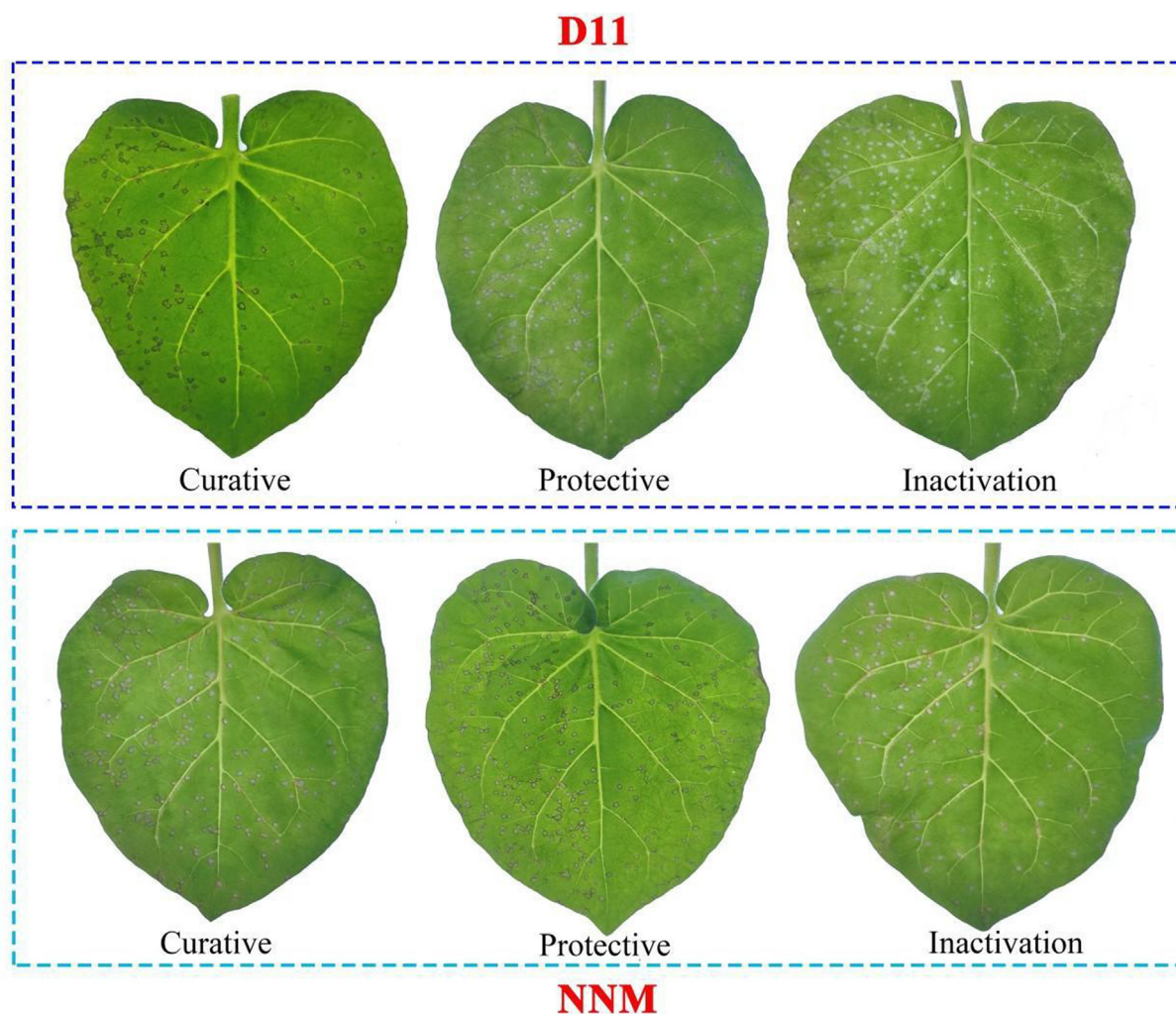


Fig. 3 Against TMV activities of **D11** and **NNM** *in vivo*.

Table 2 EC₅₀ values of some of the target compounds against TMV *in vivo*.

	Compounds	Toxic regression equation	r	EC ₅₀ (μg/mL) ^a
Curative	D11	$y = 1.0913x + 2.7836$	0.9773	107.4
	D12	$y = 0.8599x + 3.0692$	0.9958	175.9
	D15	$y = 0.8985x + 3.1714$	0.9671	108.4
	D16	$y = 0.8241x + 3.1336$	0.9975	184.0
	D18	$y = 0.8439x + 3.2733$	0.9889	111.2
	D22	$y = 0.8564x + 3.2726$	0.9543	104.0
	<i>NNM</i> ^b	$y = 0.9414x + 2.6527$	0.9830	311.5
	Protective	D2	$y = 0.9063x + 3.1633$	0.9346
D4		$y = 0.8776x + 3.1610$	0.9614	124.6
D10		$y = 1.0705x + 2.5815$	0.9929	181.6
D11		$y = 0.9735x + 2.7799$	0.9485	190.8
D12		$y = 0.8974x + 3.1514$	0.9568	114.8
D16		$y = 0.9464x + 3.0810$	0.9633	106.6
D18		$y = 0.8208x + 3.1481$	0.9727	180.4
<i>NNM</i> ^b		$y = 0.9289x + 2.8519$	0.9589	205.4

^a Average of three replicates, ^b The commercial antiviral agent. Ningnanmycin (NNM).

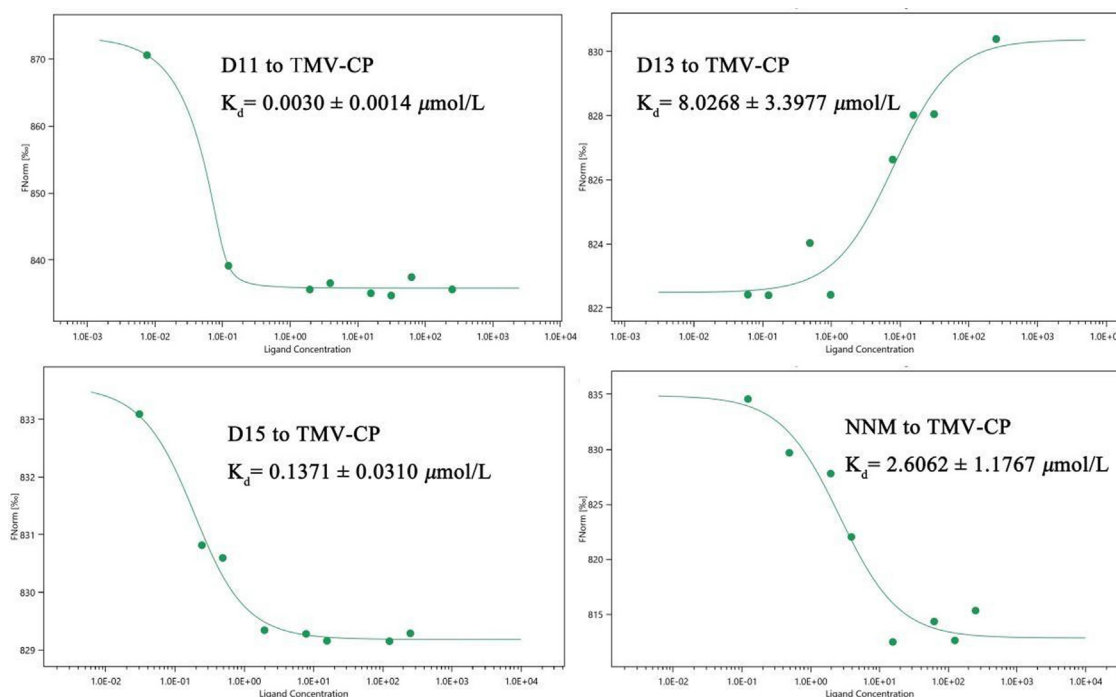


Fig. 4 MST results of **D11**, **D13**, **D15** and **NNM**.

inhibitory activity against TMV-CP. Although the commercial drug **NNM** formed two hydrogen bonds with amino acid residue **GLU-306** (3.0 Å), and the total binding free energy was -1.05 kcal/mol, which shows that the affinity with TMV protein was **D11** > **NNM**. In contrast, **D13** formed only one hydrogen bond with residue **ASN-127** (3.0 Å), the total binding free energy was -5.29 kcal/mol, forming three hydrophobic bonds, the effect of hydrogen bonding in molecular docking was most obvious, so the affinity with TMV protein was **D13** < **NNM**. In conclusion, the order of binding ability with TMV protein was **D11** > **NNM** > **D13**, which is consistent with the results of the preliminary screening data.

3.5. Effects of **D11** on defensive enzyme activities

Peroxidase (POD) has the dual effect of eliminating the toxicity of peroxyphenols and amines in plants. The changes of POD content in tobacco after treatment with **D11** are shown in Fig. 6. The POD content gradually increased in all groups during 1–7 d of TMV inoculation, the POD content in the **D11** + TMV group reached the highest value at 7 d, which was 110% higher than that in the CK + TMV group during the corresponding period. In addition, the POD content of the **D11** + TMV group was higher than that of the

CK + TMV group from 1 to 7 d. The POD content of the **D11** group was higher than that of the CK group during 2–7 d. The above experimental results showed that **D11** could increase POD to a certain extent and improve the disease resistance of plants, which in turn inhibited the virus infestation.

Succinate dehydrogenase (SDH), a marker enzyme of mitochondria, is one of the hubs linking oxidative phosphorylation and electron transfer, its activity can generally be used as an indicator to evaluate the degree of operation of the tricarboxylic acid cycle. The changes of SDH content in tobacco after **D11** treatment are shown in Fig. 6. After inoculation with TMV, the SDH content in tobacco treated with **D11** gradually increased during the 1–3 d and reached the highest value in the 3 d, then decreased during the 3–7 d. In the 3 d, the SDH content of the **D11** + TMV group was much higher than that of the CK + TMV group by 63%, and the SDH content of the **D11** + TMV group was higher than that of the CK + TMV group in the 1–7 d. The SDH content of the **D11** group gradually increased during 1–5 d and reached the highest value at 5 d, decreasing during 5–7 d. At 5 d, the SDH content of the **D11** group was 17% higher than that of CK group. The SDH content of **D11** was higher than that of the CK group from 1 to 5 d. It was shown that **D11** could improve the disease resistance of plants against virus particles, thus reducing the symptoms of tobacco plants.

3.6. Malondialdehyde content analysis

Malondialdehyde (MDA) content reflects the degree of membrane lipid peroxidation caused by tobacco infestation. As shown in Fig. 7, after TMV inoculation, MDA content in tobacco treated with **D11** decreased gradually from the 1–5 d, reached the lowest value at the 5 d, and increased from the 5 to 7 d. Especially at the 5 d, the MDA content in the **D11** + TMV group was much lower than that in the

Table 3 Molecular docking datas of **D11**, **D23**, **NNM**.

Compounds	AA-Residues	Binding-Energy(kcal/mol)	Distance
D11(A)	ASP-70	-7.44 kcal/mol	3.8 Å
	SER-215		3.0 Å
D13(B)	ASN-127	-5.29 kcal/mol	3.0 Å
NNM(C)	GLU-306	-1.05 kcal/mol	3.0 Å
	GLU-306		3.0 Å

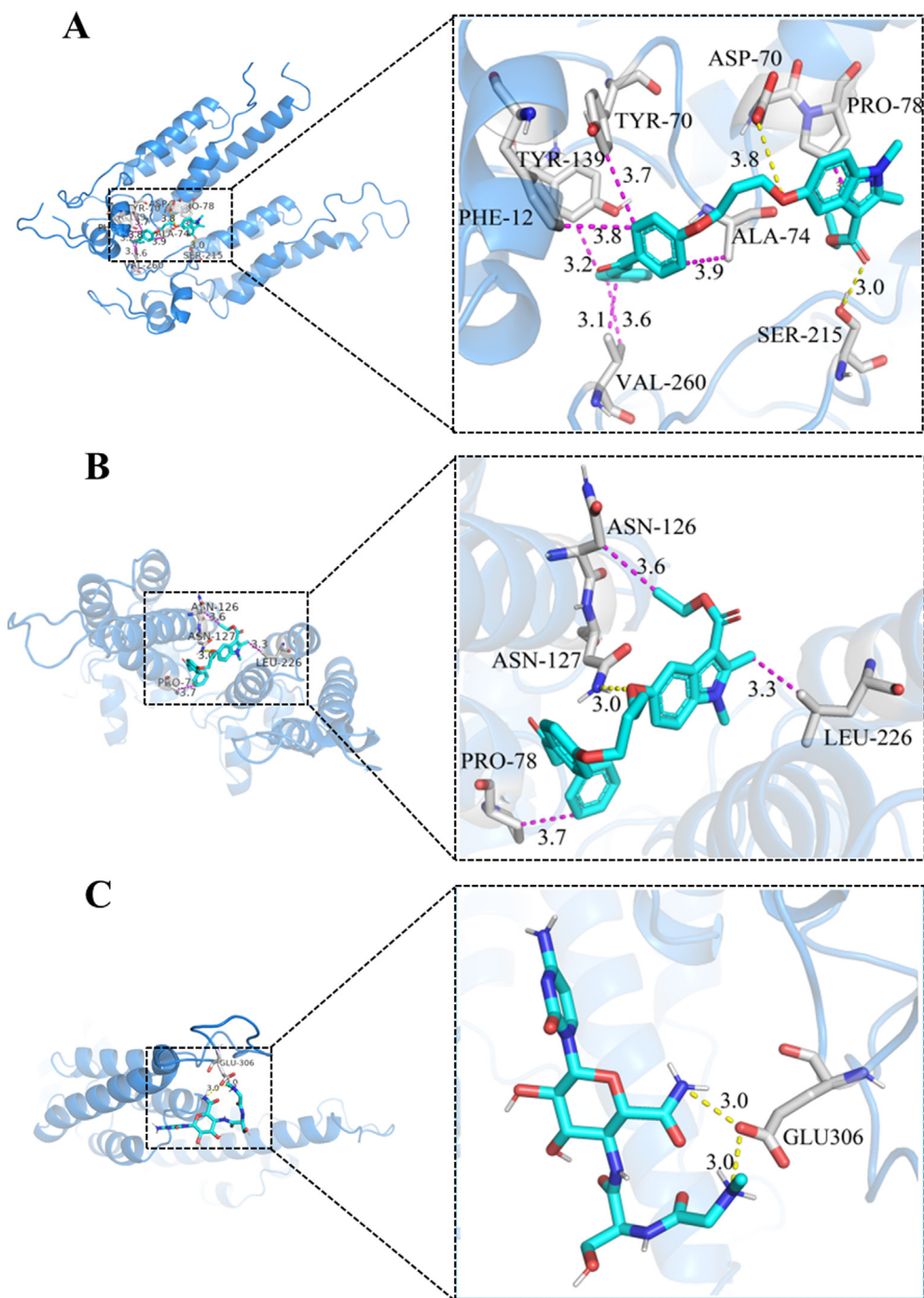


Fig. 5 Molecular docking results of **D11** (A), **D13** (B) and **NNM** (C).

CK + TMV group by about 60%. In addition, the MDA content in the **D11** group was less than that in the CK group during the period 1–7 d. Thus, it can be concluded that **D11** can reduce the MDA content in tobacco plants, effectively prevent TMV infestation and reinfestation, improve the disease resistance of tobacco.

3.7. Antibacterial activity of **D1–D24**

The inhibitory activities of the synthesized target compounds against *Xoo*, *Xac*, and *Psa* were determined at the concentra-

tion of 100 $\mu\text{g/mL}$ and 50 $\mu\text{g/mL}$. The results of the tests are shown in Table 4. Some compounds showed inhibitory activity against both *Xac* and *Xoo*. At a concentration of 100 $\mu\text{g/mL}$, **D18** showed 71.2% inhibition of *Xac*, which was better than the commercial drugs thiodiazole copper (61.5%) and bismethiazol (41.2%), **D23** showed 68.2% inhibition of *Xoo*, which was higher than the commercial drugs thiodiazole copper (60.6%) and bismethiazol (49.3%). At 50 $\mu\text{g/mL}$, **D18** inhibited *Xac* by 60.0%, which was superior to thiodiazole copper (42.1%) and bismethiazol (33.2%), **D23** inhibited *Xoo* by 52.8%, which was superior to thiodiazole copper (32.7%) and bismethiazol (26.0%).

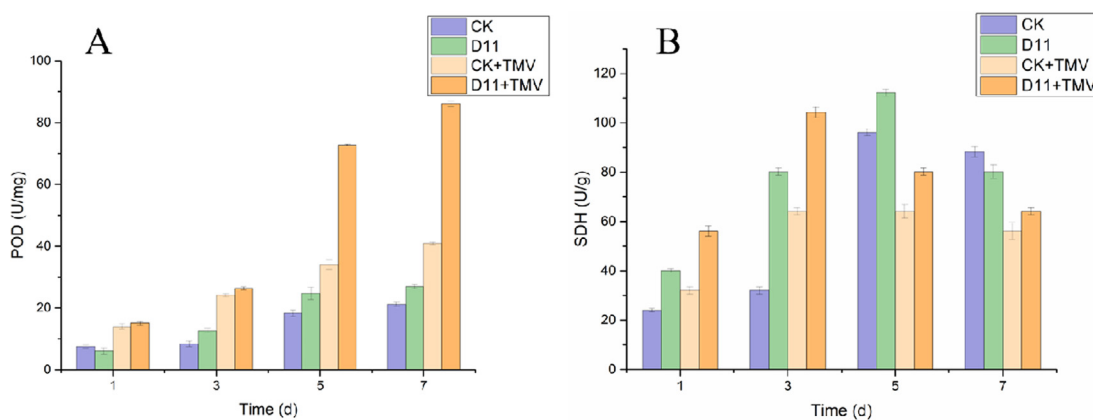


Fig. 6 Effects of **D11** on POD(A) and SDH(B) activity in tobacco leaves. Vertical bars refer to mean Standard Deviation (n = 3).

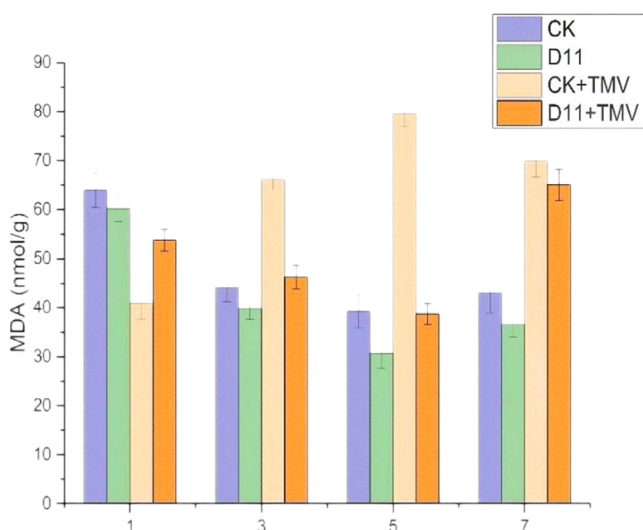


Fig. 7 Effects of **D11** on MDA content in tobacco. Vertical bars refer to mean Standard Deviation (n = 3).

To further confirm the results obtained from the initial screening, the EC_{50} values of some compounds for bacterial inhibition were tested and the results are shown in Table 5, **D18** gave an EC_{50} value of 40.2 $\mu\text{g/mL}$ for *Xac*, which was superior to the commercial drugs thiodiazole copper (60.8 $\mu\text{g/mL}$) and bismethiazol (101.9 $\mu\text{g/mL}$). The EC_{50} value of **D23** for *Xoo* was 50.3 $\mu\text{g/mL}$, which was better than that of thiodiazole copper (79.8 $\mu\text{g/mL}$) and bismethiazol (106.2 $\mu\text{g/mL}$).

According to the bacterial inhibitory activities shown in Table 4, The structure–activity relationship (SAR) analysis showed that the inhibitory activities of **D18** (n = 4, R = 3-Br-Ph) and **D6** (n = 3, R = 3-Br-Ph) against *Xac* were 71.2 and 11.0%, at a concentration of 100 $\mu\text{g/mL}$. Indicating that the growth of *Xac* could be inhibited when the number of C atoms of brominated alkanes was 4. In addition, when R was electron-absorbing group can enhance the inhibition rate of the compounds against *Xac*, such as **D18** (n = 4, R = 3-Br-Ph) showed significantly higher inhibition rate than **D16** (n = 4, R = 3-CH₃-Ph), the effect of introducing heterocyclic groups was analyzed, such as **D19** (n = 4, R = 2-Thienyl)

showed higher inhibition rate than **D20** (n = 4, R = 4-OCH₃-Ph), indicating that the introduction of heterocyclic groups contributes to the inhibition of *Xac* activity. Similarly, the structure activity relationship of the compounds on *Xoo* inhibition was analyzed at 100 $\mu\text{g/mL}$ concentration, the inhibition rate of **D23** (n = 4, R = 4-CH₃-Ph) was 68.2%, significantly higher than that of **D16** (n = 4, R = 3-CH₃-Ph), where R of **D23** was *para*-substituted phenyl and R of **D16** was *m*-substituted phenyl, thus, it is clear that when R is a *para*-electron giving substituent group, it is beneficial to improve the *Xoo* inhibiting activity. In addition, the inhibition rate of **D23** and **D11** was **D23** (n = 4, R = 4-CH₃-Ph) > **D11** (n = 3, R = 4-CH₃-Ph), suggesting that when the number of C-atoms of brominated alkanes was 4, the inhibition of *Xoo* was also enhanced.

3.8. Effect of **D23** on the hyphae morphology of *Xoo*

The mechanism of action of **D23** on *Xoo* was further investigated by SEM. As shown in the Fig. 8, the cells in the CK group without drug treatment were uniformly full and showed a complete cylindrical shape. After treatment with **D23**, at 50 $\mu\text{g/mL}$, some of the cells were flattened and the cell membrane was ruptured, at 100 $\mu\text{g/mL}$, cell rupture increased significantly, exhibiting contraction, collapse and deformation. SEM analysis showed that the greater the drug concentration, the greater the degree of cell membrane damage, which further suggests that **D23** can disrupt cell membranes and has potential antibacterial effects.

4. Conclusions

In this study, a series of chalcone derivatives containing indole were synthesized and their structures were characterized. The results of biological assays showed that some of the target compounds exhibited excellent antiviral and antibacterial activities. Among them, **D11** surpassed the commercial drug NNM in terms of both Curative and protective activities. The Molecular docking, MST, MDA, POD and SDH assays were performed on **D11**, the results of mechanism of action were consistent with the preliminary screening datas. The inhibitory activity of the **D23** against *Xoo* was tested by 96-well plate assay, and the test results showed that **D23** had excellent inhibitory effect on *Xoo*, and scanning electron microscopy experiments were performed. This study lays the foundation for the application of chalcone derivatives in pesticides.

Table 4 Antibacterial activity of the target compounds **D1-D24**.

Compounds	Inhibition rate (%) ^a					
	<i>Xac</i>		<i>Psa</i>		<i>Xoo</i>	
	100 µg/mL	50 µg/mL	100 µg/mL	50 µg/mL	100 µg/mL	50 µg/mL
D1	7.8 ± 0.7	8.0 ± 2.9	36.8 ± 2.8	30.8 ± 4.5	17.4 ± 4.1	17.6 ± 4.0
D2	5.7 ± 2.0	7.0 ± 1.2	46.0 ± 2.2	43.7 ± 0.5	20.9 ± 1.9	10.9 ± 1.8
D3	13.4 ± 2.0	14.3 ± 1.3	44.1 ± 4.3	40.8 ± 1.7	19.3 ± 3.8	19.4 ± 3.7
D4	12.9 ± 0.2	8.2 ± 0.9	28.4 ± 3.0	33.9 ± 2.5	4.6 ± 2.6	2.5 ± 0.7
D5	16.0 ± 4.6	7.9 ± 4.5	42.6 ± 2.9	35.0 ± 0.2	13.4 ± 2.5	19.6 ± 2.5
D6	11.0 ± 0.8	8.7 ± 1.6	34.6 ± 3.8	29.8 ± 3.5	4.7 ± 2.2	24.6 ± 2.9
D7	1.9 ± 1.4	4.4 ± 1.2	36.5 ± 2.3	40.1 ± 3.0	22.5 ± 0.5	24.2 ± 0.5
D8	10.1 ± 0.6	10.1 ± 3.5	5.7 ± 2.2	33.2 ± 1.6	28.3 ± 0.7	26.6 ± 0.7
D9	16.6 ± 1.6	13.3 ± 2.1	19.2 ± 3.4	13.2 ± 1.1	18.7 ± 0.1	9.1 ± 1.7
D10	14.5 ± 1.3	15.9 ± 2.1	23.9 ± 1.6	17.6 ± 2.9	13.5 ± 2.1	17.2 ± 2.2
D11	14.1 ± 0.5	13.2 ± 2.7	34.3 ± 0.6	22.5 ± 3.4	9.6 ± 0.9	23.8 ± 1.7
D12	18.9 ± 1.6	14.5 ± 2.4	26.9 ± 4.8	29.9 ± 2.5	6.9 ± 2.1	7.5 ± 4.0
D13	13.5 ± 2.8	10.7 ± 2.0	27.1 ± 1.5	27.9 ± 3.0	14.8 ± 0.2	24.5 ± 0.6
D14	13.9 ± 1.1	16.4 ± 3.7	26.4 ± 1.9	13.9 ± 3.3	15.8 ± 1.2	13.7 ± 1.7
D15	14.0 ± 0.8	13.8 ± 0.9	35.4 ± 2.4	20.6 ± 4.0	16.4 ± 0.5	15.6 ± 2.4
D16	14.9 ± 0.4	13.6 ± 0.2	15.4 ± 1.2	15.3 ± 2.0	31.5 ± 1.4	21.1 ± 2.2
D17	22.2 ± 0.4	3.4 ± 2.6	34.2 ± 4.0	11.1 ± 1.3	40.3 ± 0.9	29.5 ± 2.1
D18	71.2 ± 1.4	60.0 ± 0.4	33.1 ± 2.7	20.6 ± 2.1	40.0 ± 3.8	30.9 ± 2.0
D19	64.2 ± 0.4	14.7 ± 1.3	23.5 ± 2.5	29.4 ± 0.7	33.8 ± 3.5	30.4 ± 2.1
D20	53.2 ± 3.1	22.7 ± 3.9	28.3 ± 1.7	18.9 ± 2.5	21.1 ± 0.8	24.1 ± 0.2
D21	41.9 ± 2.7	24.9 ± 0.5	31.3 ± 2.0	10.6 ± 1.4	7.8 ± 0.8	21.5 ± 1.3
D22	23.9 ± 1.9	0.9 ± 1.8	40.5 ± 0.8	13.2 ± 1.6	29.4 ± 0.2	28.2 ± 2.7
D23	5.7 ± 0.9	8.1 ± 2.9	25.1 ± 4.5	27.1 ± 2.6	68.2 ± 1.7	52.8 ± 0.2
D24	6.0 ± 4.5	15.7 ± 0.7	17.1 ± 2.5	5.5 ± 1.0	16.9 ± 0.7	14.6 ± 1.7
<i>Bismertiazol</i> ^b	41.2 ± 1.9	33.2 ± 3.4	49.8 ± 2.4	38.4 ± 3.1	49.3 ± 3.2	26.0 ± 2.7
<i>Thiodiazole copper</i> ^b	61.5 ± 0.2	42.1 ± 1.6	61.5 ± 0.5	47.2 ± 3.8	60.6 ± 0.8	32.7 ± 0.4

^a Average of three replicates, ^b The Commercial anti-bacterial agents.

Table 5 The EC₅₀ values of several target compounds against *Xac* and *Xoo*.

Compounds	Toxic regression equation	r	EC ₅₀ (µg/mL) ^a
<i>Xac</i>	D18	$y = 0.9279x + 3.5119$	0.9396
	<i>Bismertiazol</i> ^b	$y = 0.7952x + 3.4030$	0.9745
	<i>Thiodiazole copper</i> ^b	$y = 0.6306x + 3.8749$	0.9376
<i>Xoo</i>	D23	$y = 1.0131x + 3.2763$	0.9962
	<i>Bismertiazol</i> ^b	$y = 0.8603x + 3.2570$	0.9863
	<i>Thiodiazole copper</i> ^b	$y = 0.6147x + 3.8307$	0.9498

^a Average of three replicates, ^b The Commercial anti-bacterial agents.



Fig. 8 SEM of the hyphae of *Xoo* with or without compound **D23** treatment. (A) CK groups (DMSO); (B) **D23** at 50 µg/ mL and (C) **D23** at 100 µg/ mL.

Declaration of Competing Interest

The authors declare that they have no known competing financial interests or personal relationships that could have appeared to influence the work reported in this paper.

Acknowledgement

The authors gratefully acknowledge the National Nature Science Foundation of China (No. 32072446), the Science Foundation of Guizhou Province (No. 20192452).

Supporting information.

The Supporting Information includes the characterization data, HNMR and HRMS spectrogram for the target compounds.

Appendix A. Supplementary data

Supplementary data to this article can be found online at <https://doi.org/10.1016/j.arabjc.2023.104776>.

References

- Bale, A.T., Salar, U., Khan, K.M., Chigurupati, S., Fasina, T., Ali, F., Ali, M., Nanda, S.S., Taha, M., Perveen, S., 2021. Chalcones and bischalcones analogs as DPPH and ABTS radical scavengers. *Lett. Drug. Des. Discov* 18, 249–257.
- Chandrabose, K., Narayana, S.H., Narayana, M., Sakthivel, R., Uma Vanam, E., Manivannan, D.K., 2014. Advances in chalcones with anticancer activities. *Recent. Pat. Anti-canc.* 10, 97–115.
- Chao, S.J., 2019. The orientation and policy suggestions for the agricultural high-quality development. *J. Manage.* 32, 28–35.
- Chen, Y., Li, P., Chen, M., He, J., Su, S.J., He, M., Wang, H., Xue, W., 2020. Synthesis and antibacterial activity of chalcone derivatives containing thioether triazole. *J. Heterocyclic. Chem.* 57, 983–990.
- Claudio, A., Manuel, A., Kevin, B., Christian, V., Jorge, S., Marcelo, K., 2018. Industrial prune processing and its effect on pesticide residue concentrations. *Food. Chem.* 268, 264–270.
- Ding, C.F., Ma, H.X., Yang, J., 2018. Antibacterial indole alkaloids with complex heterocycles from *voacanga africana*. *Org. Lett.* 20, 2702–2706.
- Ding, X., Xu, Y.B., Yan, L.L., Chen, L., Lu, Z.J., Ge, C.Y., Zhao, X. Y., Wang, Z.W., Lu, A.D., Wang, Q.M., 2022. Marine sesquiterpenes for plant protection: discovery of laurene sesquiterpenes and their derivatives as novel antiviral and antifungal agents. *J. Agric. Food Chem.* 70, 6006–6014.
- Fu, Y., Liu, D., Gan, X.H., 2020. New chalcone derivatives: synthesis, antiviral activity and mechanism of action. *RSC Advances.* 10, 24483–24490.
- Gan, X.H., Wang, Z.X., Hu, D.Y., 2021. Synthesis of novel antiviral ferulic acid–eugenol and isoeugenol hybrids using various link reactions. *J. Agric. Food Chem.* 69, 13724–13733.
- Guan, L.J., Zhao, L.H., Dong, R.F., 2014. The influence of isobavachalcone to cellular structure and mycelial morphology of *valsa mali* miyabe et yamada. *Agrochemicals.* 53, 290–292.
- Hiroyuki, S., Yoshinori, H., Satoshi, N., Hitoshi, A., Kazuki, K., 2003. Simultaneous determination of all polyphenols in vegetables, fruits, and teas. *J. Agric. Food Chem.* 51, 571–581.
- Huang, E., Zhang, L., Xiao, C.Y., Meng, G.P., Zhang, B.Q., Hu, J.S., Wan, D.C., Meng, Q.G., Jin, Z., Hu, C., 2019. Synthesis and biological evaluation of indole-3-carboxamide derivatives as antioxidant agents. *Chinese. Chem. Lett.* 30, 2157–2159.
- Ibrahim, T.S., Moustafa, A.H., Almalki, A.J., Allam, R.M., Althagafi, A., Md, S., Mohamed, M.F., 2021. Novel chalcone/aryl carboximidamide hybrids as potent anti-inflammatory via inhibition of prostaglandin E2 and inducible NO synthase activities: design, synthesis, molecular docking studies and ADMET prediction. *J. Enzym. Inhib. Med. Chem.* 36, 1067–1078.
- Jiang, S.C., Tang, X., Chen, M., He, J., Su, S.J., Liu, L.W., He, M., Xue, W., 2020. Design, synthesis and antibacterial activities against *Xanthomonas oryzae* pv. *oryzae*, *Xanthomonas axonopodis* pv. *Citri* and *Ralstonia solanacearum* of novel myricetin derivatives containing sulfonamide moiety. *Pest Manag. Sci.* 76, 853–860.
- José, T.D., Sylvia, P.D., Francisco, D.V., 2018. Synthesis of leading chalcones with high antiparasitic, against *hymenolepis nana*, and antioxidant activities. *Braz. J. Pharm. Sci.* 54, 2175–2179.
- Kang, J., Gao, Y., Zhang, M., 2020. Streptindole and its derivatives as novel antiviral and anti-phytopathogenic-fungus agents. *J. Agric. Food Chem.* 68, 7839–7849.
- Li, Y.Y., Zhou, X., Li, S.M., Zhang, Y.P., Yuan, C.M., He, S.Z., Yang, Z.C., Yang, S., Zhou, K., 2022. Increasing structural diversity of prenylated chalcones by two fungal prenyl transferases. *J. Agric. Food Chem.* 70, 1610–1617.
- Li, C.J., Zhu, H.M., Li, C.Y., Qian, H., Yao, W.R., Guo, Y.H., 2021. The present situation of pesticide residues in china and their removal and transformation during food processing. *Food. Chem.* 354, 129552.
- Lin, L.P., Tan, R.X., 2018. Bioactive alkaloids from indole-3-carbinol exposed culture of *daldiniaeschscholzii*. *Chinese. J. Chem.* 36, 749–753.
- Liu, H.B., Lauro, G., Connor, R.D., 2017. Tulongicin, an antibacterial tri-indole alkaloid from a deep-water topsentia sp. sponge. *J. Nat. Prod.* 80, 2556–2560.
- Liu, T.T., Peng, F., Cao, X., Liu, F., Wang, Q.F., Liu, L.W., Xue, W., 2021. Design, synthesis, antibacterial activity, antiviral activity, and mechanism of myricetin derivatives containing a quinazolinone moiety. *ACS Omega.* 6, 30826–30833.
- Liu, T.T., Peng, F., Zhu, Y.Y., Cao, X., Wang, Q.F., Liu, F., Liu, L. W., Xue, W., 2022. Design, synthesis, biological activity evaluation and mechanism of action of myricetin derivatives containing thioether quinazolinone. *Arab. J. Chem.* 15, 104019.
- Liu, Z.G., Tang, L.G., Zhu, H.P., Xu, T.T., Qiu, C.Y., Zheng, S.Q., Gu, Y.G., Feng, J.P., Zhang, Y.L., Liang, G., 2016. Design, synthesis, and structure–activity relationship study of novel indole-2-carboxamide derivatives as anti-inflammatory agents for the treatment of sepsis. *J. Med. Chem.* 59, 4637–4650.
- Mariana, R.M., Octávio, L.F., 2022. CRISPR/Cas: The new frontier in plant improvement. *ACS Agric. Sci. Technol.* 2, 202–214.
- Marqués, M.C., Javier, S.V., Raúl, R., Roser, M.M., Rosa, M.C., Gustavo, G., Alberto, C., José, A.D., Guillermo, R., 2022. Diagnostics of infections produced by the plant viruses TMV, TEV, and PVX with CRISPR-Cas12 and CRISPR-Cas13. *ACS Synth. Biol.* 11, 2384–2393.
- Nadia, A.A., Elkanzi, H.H., Ruba, A., Alolayan, W.D., Fatin, M., Rania, B.B., 2022. Synthesis of chalcones derivatives and their biological activities: A Review. *ACS Omega.* 7, 27769–27786.
- Nurkenov, O., Ibraev, M., Schepetkin, I., Khlebnikov, A., Seilkhanov, T., Arinova, A., Isabaeva, M., 2019. Synthesis, structure, and anti-inflammatory activity of functionally substituted chalcones and their derivatives. *Russ. J. Gen. Chem.* 89, 1360–1367.
- Palassini, E., Frezza, A.M., Mariani, L., 2017. Long-term efficacy of methotrexate plus vinblastine / vinorelbine in a large series of patients affected by desmoid-type fibromatosis. *Cancer J.* 23, 86–91.
- Peng, F., Liu, T.T., Wang, Q.F., Liu, F., Cao, X., Yang, J.S., Liu, L. W., Xie, C.W., Xue, W., 2021. Antibacterial and antiviral activities of 1,3,4-oxadiazole thioether 4H-chromen-4-one derivatives. *J. Agric. Food Chem.* 69, 11085–11094.

- Qin, X.J., Zhao, Y.L., Lunga, P.K., 2015. Indole alkaloids with antibacterial activity from aqueous fraction of *alstonia scholaris*. *Tetrahedron*. 71, 4372–4378.
- Quan, V.V., Adam, M., 2020. In silico study of the radical scavenging activities of natural indole-3-carbinols. *J. Chem. Inf. Model.* 60, 316–321.
- Tang, X.M., Zhou, Q., Zhan, W.L., Hu, D., Zhou, R., Sun, N., Chen, S., Wu, W.N., Xue, W., 2022. Synthesis of novel antibacterial and antifungal quinoxaline derivatives. *RSC Advances*. 12, 2399–2407.
- Wang, Q., Song, H.J., Wang, Q.M., 2021. Studies on the biological activity of gem-difluorinated 3, 3'-spirocyclic indole derivatives. *Chinese. Chem. Lett.* 8, 1–4.
- Wei, X., Yang, J., Ma, H.X., 2018. Antimicrobial indole alkaloids with adductive C9 aromatic unit from *gelsemium elegans*. *Tetrahedron Lett.* 59, 2066–2070.
- Wu, S.W., Shi, Z.Y., Chen, X.N., Gao, J.K., Wang, X.G., 2022. Arbuscular mycorrhizal fungi increase crop yields by improving biomass under rainfed condition: a meta-analysis. *Peer J.* 10, 12861.
- Xie, J.L., Xu, W.T., Wang, Q.M., 2020. Synthesis and antiviral/fungicidal/insecticidal activities study of novel chiral indole diketopiperazine derivatives containing acylhydrazone moiety. *J. Agric. Food Chem.* 68, 5555–5571.
- Xu, Z., Zhang, S., Song, X., 2017. Design, synthesis and invitro antimycobacterial evaluation of *gatifloxacin-1H-1,2,3-triazole-isatin* hybrids. *Bioorg. Med. Chem. Lett.* 227, 3643–3646.
- Xu, F., Zhang, L., Zhou, X.B., Guo, X.Y., Zhu, Y.C., Liu, M., Xiong, H., Jiang, P., 2021. The ratoon rice system with high yield and high efficiency in china: progress, trend of theory and technology. *Field. Crop. Res.* 272, 108282.
- Yan, S.Y., Weng, B.S., Jing, L.J., 2021. Research progress on the effect of drought on root system of summer maize. *IOP Conf. Ser.: Earth Environ. Sci.* 705, 012003.
- Yang, O.Y., Li, J., Chen, X., Fu, X., Sun, S., Wu, Q., 2021. Chalcone derivatives: role in anticancer therapy. *Biomolecules*. 11, 894–930.
- Ye, Y.Q., Dong, W., Liu, C., Lei, P., Shen, Q.P., Yang, J.X., Wang, Y. D., Zhou, K., Ji, B.K., Gao, X.M., Zhou, M., Hu, Q.F., 2016. Changes in *gastrodia tuber* ethanol extracts during *grifola frondosa* fermentation. *Chem. Nat. Compd.* 52, 1–4.
- Zahrani, N.A., El-Shishtawy, R.M., Elaasser, M.M., Asiri, A.M., 2020. Synthesis of novel chalcone-based phenothiazine derivatives as antioxidant and anticancer agents. *Molecules*. 25, 4566–4581.
- Zhang, Z.X., Wang, H.Y., Wang, K.Y., Jiang, L.L., Wang, D., 2017. Use of lentinan to control sharp eyespot of wheat, and the mechanism involved. *J. Agric. Food Chem.* 65, 10891–10898.
- Zhao, X., Cui, H.X., Wang, Y., Sun, C.J., Cui, B., Zeng, Z.H., 2018. Development strategies and prospects of nano-based smart pesticide formulation. *J. Agric. Food Chem.* 66, 6504–6512.
- Zhou, Q., Tang, X.M., Chen, S., Zhan, W.L., Hu, D., Zhou, R., Sun, N., Wu, Y.J., Xue, W., 2022. Design, synthesis, and antifungal activity of novel chalcone derivatives containing a piperazine fragment. *J. Agric. Food Chem.* 70, 1029–1036.